Journal of Ethnopharmacology 278 (2021) 114298

Contents lists available at ScienceDirect

Journal of Ethnopharmacology

journal homepage: www.elsevier.com/locate/jethpharm

Transcriptomic study of the mechanism by which the Kai Yu Zhong Yu recipe improves oocyte quality in a stressed mouse model

Xiaoli Zhao [a,1], Ruihong Ma [a,1], Xiaoyu Zhang [a,2], Baojuan Wang [a,2], Beilei Rong [a], Nan Jiang [a], Weihua Feng [a], Mingli Chen [a], Zhipeng Huo [b], Shuming Li [c], Tian Xia [a,*]

[a] Reproductive Center, First Teaching Hospital of Tianjin University of Traditional Chinese Medicine, And National Clinical Research Center for Chinese Medicine Acupuncture and Moxibustion, Tianjin, 300381, China
[b] School of Chinese Materia Medica, Tianjin University of Traditional Chinese Medicine, Tianjin, 301617, China
[c] School of Chemical Engineering and Technology, Hebei University of Technology, Tianjin, 300130, China

ARTICLE INFO

Keywords:
Stress
Infertility
Oocyte quality
Mitochondria
Respiratory chain
ATP synthesis
Transcriptomics
Traditional Chinese medicine

ABSTRACT

Ethnopharmacological relevance: The Kai Yu Zhong Yu recipe (KYZY) is a classic herbal formula in traditional Chinese medicine (TCM) that has been used to treat infertility associated with psychological stress for more than three hundred years.

Aim of the study: Psychological stress has major impacts on fertility, with variable outcomes depending on the nature, strength, and duration of the stress. Stress can directly disturb ovulation, oocyte quality, maturation, and embryo development. The aim of this study is to investigate the molecular mechanism by which KYZY improves oocyte developmental potential under psychological stress.

Materials and methods: ICR female mice aged 4–5 weeks were randomly divided into five groups: control, stressed in the chronic unpredictable stress model (CUSM), and stressed plus KYZY treatment at 38.2 g/kg (KYZYH), 19.1 g/kg (KYZYM), or 9.6 g/kg (KYZYL). Ovary function was assessed by measuring serum levels of estradiol (E2), luteinizing hormone (LH), follicle-stimulating hormone (FSH), and anti-Müllerian hormone (AMH). Oocyte quality was evaluated in terms of reactive oxygen species (ROS) levels, apoptotic DNA fragmentation, and mitochondria distribution. We used RNA sequencing (RNAseq) to identify differentially expressed genes (DEGs) between groups and then further analyzed the DEGs for gene ontology (GO) term enrichment and protein-protein interactions.

Results: Mice in the stressed group had reduced serum E2, LH, and FSH as well as increased ROS levels, increased apoptosis, and disturbed mitochondria distribution in oocytes. Treatment with KYZY at all three doses reversed or ameliorated these negative effects of stress. DEG analysis identified 187 common genes between the two comparisons (stressed vs. control and KYZYM vs. stressed), 33 of which were annotated with six gene ontology (GO)'s biological process (BP) terms: cell differentiation, apoptosis, ATP synthesis, protein homo-oligomerization, neuron migration, and negative regulation of peptidase activity. Protein-protein interaction network analysis of DEGs identified key hub genes. Notably, the genes *Atp5o* and *Cyc1* were both involved in the ATP synthesis and among the top three hub genes, suggesting that regulation of oocyte mitochondrial electron transport and ATP synthesis is important in the response to stress and also is a possible mechanism of action for KYZY.

Conclusions: KYZY was effective in ameliorating the adverse effects of stress on oocyte competence, possibly by targeting the mitochondrial respiratory chain and ATP synthase.

* Corresponding author. Reproductive Center, First Teaching Hospital of Tianjin University of Traditional Chinese Medicine and National Clinical Research Center for Chinese Medicine Acupuncture and Moxibustion, 88 Changling Road, Xiqing District, Tianjin 300381, China.
E-mail address: xiatian76@163.com (T. Xia).
[1] These authors contributed equally to this work.
[2] These authors contributed equally to this work.

https://doi.org/10.1016/j.jep.2021.114298
Received 27 January 2021; Received in revised form 26 April 2021; Accepted 1 June 2021
Available online 4 June 2021

List of abbreviations

AMH	anti-Müllerian hormone
ANOVA	one-way analysis of variance
ATCH	adrenocorticotropic hormone
BP	biological processes
CE	collision energy
COC	cumulus oocyte complexes
CORT	cortisol
CRH	corticotropin-releasing hormone
CUSM	chronic unpredictable stress model
DAVID	Database for Annotation, Visualization and Integrated Discovery
DCFH-DA	2′,7′-dichlorodihydrofluorescein diacetate
DEGs	differentially expressed genes
E2	estradiol
ELISA	enzyme-linked immunosorbent assay
FSH	follicle-stimulating hormone
GEO	Gene Expression Omnibus
GO	gene ontology
GSH	glutathione
HCG	human chorionic gonadotropin
HPA	hypothalamic-pituitary-adrenal
HPO	hypothalamic-pituitary-ovarian
HSD	Honest Significant Difference
KYZY	Kai Yu Zhong Yu recipe
LH	luteinizing hormone
MCC	Maximal Clique Centrality
MII	second metaphase stage
NCBI	National Center for Biotechnology Information
OS	oxidative stress
OXPHOS	oxidative phosphorylation
PMSG	pregnant mare serum gonadotrophin
PPI	protein-protein interaction
RCF	relative centrifugal force
RNAseq	RNA sequencing
ROS	reactive oxygen species
TCM	traditional Chinese medicine
TdT	terminal deoxynucleotidyl transferase
TUNEL	terminal deoxynucleotidyl transferase dUTP nick end labeling
UniProt	Universal Protein Resource
UPLC-HRMS	ultra-high performance liquid chromatography coupled with high-resolution mass spectrometry

1. Introduction

Infertility is a major issue in reproductive medicine that has complex etiologies. The negative effects of psychological stress, especially at high levels, on conception and IVF outcome have gained much attention (Ebbesen et al., 2009; Louis et al., 2011). Maternal psychological stress is also reported to increase the risk of miscarriages (Nepomnaschy et al., 2006) and stress has been defined as a negative stimulator that can retard development (Puscheck et al., 2018). Thus, understanding the physiological effects of psychological stress on infertility is important.

Oocyte defects are a major cause of abnormal embryo development and infertility. Increasing evidence shows that psychological stress exerts deleterious effects on oocyte quality at multiple levels. The hypothalamic-pituitary-ovarian (HPO) axis is the main endocrine regulator of oocyte maturation, fertilization, and embryo development. Stress inhibits the function of the HPO axis by activating the hypothalamic-pituitary-adrenal (HPA) axis. Increased levels of corticotropin-releasing hormone (CRH), adrenocorticotropic hormone (ATCH), and glucocorticoids suppress the secretion of luteinizing hormone (LH), estradiol (E2), and progesterone, which impairs ovulation, fertilization, and the subsequent embryo development (Kiapekou et al., 2010; Prasad et al., 2016; Toufexis et al., 2014; Valsamakis et al., 2019).

Another major negative factor that affects oocyte quality is the increased production of reactive oxygen species (ROS) that occurs under stress. ROS are second messengers that are required for normal reproductive function (Jamil et al., 2020; Prasad et al., 2016). Optimal levels of ROS are maintained by a balance of free radical generation and reactions with antioxidants. The effect of ROS on preimplantation embryo development is complex, depending on the ROS concentration, the stage of development, and the microenvironment of the embryos. Abnormally high levels of ROS lead to oxidative stress, which is harmful for oogenesis, meiosis, and ovulation. Excessive ROS production and reduced antioxidant activity are characteristics of aging oocytes and contribute to the age-related decline of oocyte developmental competence (Das et al., 2006; Peters et al., 2020; Sasaki et al., 2019). Oxidative stress, induced by ROS, is a major factor that causes IVF failure (von Mengden et al., 2020). The administration of antioxidants is beneficial for oocyte maturation, fertilization, and embryo development, and the effects are dose-dependent *in vitro* (von Mengden et al., 2020).

Mitochondria produce most of the ATP in a cell and also the majority of ROS in the body. Oocytes primarily use pyruvate and fatty acids as substrates to power mitochondrial ATP generation (Bradley and Swann, 2019). The required quantities of these substrates to be used in the oocyte mitochondria are distinctive for different species. The energy requirement of the mitochondria in oocytes and early embryos also varies according to their developmental stages. Oocytes and embryos from day 1–3 depend on oxidative phosphorylation (OXPHOS) for ATP production. From day 4, the embryos rely on aerobic glycolysis for energy and building blocks for the rapid synthesis of macromolecules. OXPHOS produces ROS as by-products. The absence of effective antioxidant mechanisms in oocytes also makes them vulnerable to ROS damage.

Oocyte competence relies on the maturation at both the cytoplasmic and nuclear levels and requires mitochondria to provide energy. In mice, most mature oocytes at the second metaphase stage (MII) have a polarized mitochondria distribution around the spindles to provide energy for the extrusion of the second polar body and fertilization (Lei et al., 2014). However, the mitochondria are mainly clustered around the pronuclei after fertilization. In aging and degenerating oocytes, the mitochondria are also clustered, suggesting their functional changes.

The Kai Yu Zhong Yu recipe (KYZY) was originated from Qingzhu Fu's Obstetrics and Gynecology, a classical monograph in traditional Chinese medicine (TCM) that was written in 1673 (Fu, 2006). It consists of Radix Paeoniae Alba, Rhizoma Cyperi, Radix Angelicae Sinensis, Rhizoma Atractylodis Macrocephalae, Cortex Moutan, Poria, and Radix Trichosanthis. KYZY has been used to treat infertility caused by, in modern medical terms, psychological stress (Cong et al., 2020; Tang, 2006; Wang, 2003; Zhang, 1983).

KYZY contains several herbs that have been shown in other TCM recipes to have antidepressant effects (Feng et al., 2016) and protect rat follicular development in the chronic unpredictable stress model (CUSM) (Xu et al., 2020). Examples include Radix Paeoniae Alba, Rhizoma Cyperi (Chang et al., 2015; Zhang et al., 2020), Angelicae Sinensis Radix, Rhizoma Atractylodis Macrocephalae, and Poria (Gao et al., 2011; Gong, W. et al., 2019). However, the molecular mechanism of KYZY is unknown. Therefore, we studied the constituents of KYZY, their effect on a mouse model of depression and the mechanism of the positive effect of KYZY on oocyte quality and early embryo development.

2. Materials and methods

2.1. KYZY preparation

The KYZY consists of 15 g Radix Angelicae Sinensis (Angelica sinensi (Oliv.) Diels), 15 g Rhizoma Atractylodis Macrocephalae (Atractylodes macrocephala Koidz.), 9 g Rhizoma Cyperi (Cyperus rotundus L.), 30 g Radix Paeoniae Alba (Paeonia lactiflora Pall), 9 g Cortex Moutan (the root bark of Paeonia × suffruticosa Andrews), 6 g Radix Trichosanthis (Trichosanthes kirilowii Maxim), and 9 g Poria (the sclerotium of the fungus Poria cocos F.A. Wolf).

To make the decoction, the KYZY dry mix was first soaked in 600 mL distilled water for 30 min, and then boiled for 30 min. The supernatant was filtered and kept separately. Three hundred and thirty milliliters of distilled water were added to the remaining residues, and boiled again for 30 min. The second supernatant was filtered and combined with the first supernatant.

The final volume of the decoction was further reduced by heating it to 100 mL for ultra-high performance liquid chromatography coupled with high-resolution mass spectrometry (UPLC-HRMS) analysis. For administration of the decoction by gavage to mice, we used an equivalent dose of 19.1 g/kg as the medium dose based on the dose translation from human to animal (Reagan-Shaw et al., 2008). The high dose (38.2 g/kg) and low dose (9.55 g/kg) were 2 and 0.5 times, respectively, the equivalent dose.

2.2. UPLC-HRMS analysis

One milliliter of KYZY decoction was diluted with 4 mL methanol, and then centrifuged at 10,000 relative centrifugal force (RCF). The supernatant was used for UPLC-HRMS analysis with a Waters ACQUITY UPLC system coupled with a SYNAPT G2 Q-Tof High-Resolution Mass Spectrometer (Waters Corporation, Milford, MA, USA). The separation was performed on an ACQUITY UPLC HSS T3 column (100 mm × 2.1 mm, 1.8 μm particle size, Waters) at 30 °C with a flow rate of 0.3 mL/min. The mobile phase, consisting of 0.1% formic acid-water (A) and acetonitrile (B), was delivered using a linear gradient program as follows: 0–2 min, 5% B; 2–4 min, 5%–20% B; 4–12 min 20%–30% B; 12–24 min, 30%–90% B; 24–25 min 90%–5% B; 25–30 min, 5% B. The injection volume was 4 μL. Positive and negative mass chromatograms were acquired on the MSE mode with parameters as follows: desolvation gas (N2): 800 L/h; cone gas: 50 L/h; desolvation temperature: 350 °C. The collision energy (CE) was set at 20–50 eV. The mass range was recorded for m/z of 50–1000.

Standard compounds were purchased from commercial venders. Arginine (B34284), paeonol (B20266), atractylenolide III (B20056), ligustilide (B20492), atractylenolide I (B20054), citrulline (B21918), gallic acid (B20851), paeoniflorin (B21148), galloylpaeoniflorin (B24590), and mudanpioside J (B32864) were from Shanghai Yuanye Bio-Technology (Shanghai, China). Oxypaeoniflora (DY0074) was from Chengdu Desite Biotech (Chengdu, China). Tryptophan (R012575) was from Rhawn Reagent (Shanghai, China).

2.3. Animals and treatment

Female ICR mice aged 4–5 weeks (Beijing Vital River Laboratory Animal Technology, Beijing, China) were maintained under standard conditions: 12 h/12 h light/dark cycle, room temperature 22 ± 2 °C, humidity 65 ± 5%. One hundred and fifty mice were randomly divided into five groups: control, stressed in CUSM, and stressed plus high dose (38.2 g/kg, KYZYH), medium dose (19.1 g/kg, KYZYM), or low dose (9.6 g/kg, KYZYL) KYZY treatment, with 30 mice in each group. Mice in the control group were not treated with any stressors or KYZY. Mice in the stressed group were exposed to random unpredictable stressors for 6 weeks (Willner, 2017; Willner et al., 1987). The stressors included swimming in the cold (13 ± 1 °C), tail pinch for 10 min, water or food deprivation for 24 h, wet bedding for 24 h, restraint for 60 min, and continuous lighting for 24 h. Mice in the KYZY groups were first treated with random unpredictable stressors for 6 weeks as in the stressed group. Subsequently they were treated with KYZY by intragastric administration of 0.1 mL of the decoction once per day for 4 weeks. The animal experiment was performed according to international, national, and institutional rules considering animal experiments. All animal study protocols were approved by the Animal Ethical and Welfare Committee of the Institute of Radiation Medicine, Chinese Academy of Medical Sciences and Peking Union Medical College, where all the animal experiments were performed (Approval Number: IRM-DWLL-2019123).

2.4. Analysis of the CUSM

2.4.1. Depressive behaviors

Mice were weighed on days 1, 6, 14, 23, 30, 37, and 42 during the CUSM procedure.

The sucrose preference test was performed at the end of CUSM to assess anhedonia induced by the stress according to previous studies (Liu et al., 2018). Briefly, each cage had one drinking bottle filled with 1% (wt/vol) sucrose (Sigma-Aldrich, Shanghai, China) on the first day, two drinking bottles filled with 1% sucrose and water, respectively, on the second day, no food and water on the third day, and again two drinking bottles with sucrose and water, respectively, on the fourth and fifth days. The positions of the two bottles on the second day were switched after 12 h to reduce any confounding effect produced by the side bias. On the final two days, both bottles were weighed before and after the experiment. The sucrose preference was calculated as the percentage of sucrose solution intake divided by the total fluid intake (sum of the water and sucrose solution consumed) x 100.

Exploratory and locomotor activities of the mice were measured using the open-field test (Himanshu et al., 2020). Mice were placed in the center of an open-field arena (50 cm × 50 cm x 40 cm, L x W x H) with a video tracking system (TM-vision, Chengdu, China) and were free to explore for 5 min. Data were collected and analyzed using OFT-100 software (TM-vision). The exploratory activity was assessed by the time spent in the center zone and the peripheral zone. The locomotor activity was assessed by the resting time, moving time, and total distance travelled. The measurement for each mouse was repeated five times.

2.4.2. Enzyme-linked immunosorbent assay (ELISA)

Blood was collected by retro-orbital bleeding. Serum was prepared from each blood sample and stored at −80 °C until analysis. Serum levels of HPA axis-associated hormones (CRH, ACTH, and cortisol (CORT)) and ovarian hormones (E2, FSH, LH, and AMH) were measured by ELISA according to the manufacturer's instructions (Shanghai Hengyuan Biotechnology, Shanghai, China).

2.5. Oocyte collection

Oocytes were collected from mice induced for super-ovulation by intraperitoneal injection with 7.5 IU pregnant mare serum gonadotrophin (PMSG, Solarbio Life Sciences, Beijing, China), followed by 7.5 IU human chorionic gonadotropin (HCG, Solarbio Life Sciences) 46 h later. Sixteen hours after the final injection, the mice were killed by cervical dislocation, and the enlarged portion of the oviducts was dissected out. Cumulus oocyte complexes (COCs) were collected under a microscope (SZX10, Olympus, Tokyo, Japan), transferred to a drop of solution containing 100 IU/mL hyaluronidase (Solarbio Life Sciences), and incubated at 37 °C for 10 min to release the granulosa cells. The oocytes were washed with PBS and used in the following experiments.

2.6. ROS measurement

The quantity of ROS in the oocytes was measured by a Reactive

Oxygen Species Assay kit (Beyotime Biotechnology, Shanghai, China). Briefly, the oocytes were incubated with 2′,7′-dichlorodihydrofluorescein diacetate (DCFH-DA) at 10 μmol/L at 37 °C for 20 min. After washing, the cells were counterstained with Hoechst 33342 for 5 min. Fluorescent images were acquired using an EVOS M7000 imaging system (Thermo Fisher Scientific, Shanghai, China) and analyzed by ImageJ software (Rueden et al., 2017).

2.7. Terminal deoxynucleotidyl transferase dUTP nick end labeling (TUNEL) assay

A TUNEL apoptosis assay kit (Beyotime Biotechnology) was used to detect DNA fragmentation in the oocytes. Briefly, the oocytes were fixed with 0.4% paraformaldehyde for 1 h, washed with PBS, and then permeabilized with 0.3% Triton X-100 for 30 min. The cells were washed again, resuspended in a staining solution containing terminal deoxynucleotidyl transferase (TdT) and FITC-labeled dUTP at a ratio of 1:9, and incubated for 60 min at 37 °C in the dark. The oocytes were washed and counterstained with 10 μg/mL DAPI (Solarbio Life Sciences) for 5 min at room temperature. Fluorescent signals were recorded by an EVOS M7000 imaging system (Thermo Fisher Scientific) and analyzed by ImageJ software (Rueden et al., 2017).

2.8. Mitochondrial fluorescent staining

Mito-Tracker Green (Beyotime Biotechnology) was used to stain the mitochondria of the oocytes at 20 nM for 30 min at 37 °C. The oocytes were washed with PBS and then stained with Hoechst 33342 to visualize the nuclei (Solarbio Life Sciences). Fluorescent images were acquired using an EVOS M7000 imaging system (Thermo Fisher Scientific) and analyzed by ImageJ software (Rueden et al., 2017).

2.9. Transcriptomic analysis

We analyzed the differential gene expression at the transcriptional level in the MII oocytes among the control, stressed, and KYZYM groups (n = 3 in each group). Fifteen oocytes were collected from each mouse, and the cDNA was synthesized directly using a SMART-Seq v4 Ultra Low Input RNA Kit (Clontech Laboratories [now Takara Bio USA], Mountain View, CA, USA) (Picelli et al., 2013). The cDNA was purified using an AMPure XP kit (Beckman Coulter, Brea, CA, USA) and validated using an Agilent 2100 Bioanalyzer with a High Sensitivity DNA Kit (Agilent, Beijing, China). A DNA library was constructed using a TruePrep DNA Library Prep Kit V2 for Illumina (Vazyme, Nanjing, China). The cDNA was fragmented and then primed by incubation with Tn5 transposase for 10 min at 55 °C. Limited-cycle PCR was performed for cDNA amplification. Subsequently, the cDNA library was purified using a SPRIselect kit (Beckman Coulter) and then quantified using a Qubit 3.0 fluorometer (Thermo Fisher Scientific). The size distribution of the library was analyzed using an Agilent 2100 Bioanalyzer. RNA sequencing (RNAseq) was performed on a Novaseq 6000 system (Illumina, San Diego, CA, USA) using a NavaSeq 6000 S4 Reagent kit (Illumina).

Raw data were filtered with TrimGalore (Bioinformatics Group at the Babraham Institute, 2019). The clean paired-end reads were aligned to the mouse reference genome 10 (GRCm38/mm10) using HISAT2 (Kim et al., 2019). Transcripts were assembled and quantified using StringTie (Kovaka et al., 2019).

The RNAseq data discussed in this publication have been deposited in NCBI's Gene Expression Omnibus (GEO) (Edgar et al., 2002) and are accessible through GEO Series accession number GSE152754 (https://www.ncbi.nlm.nih.gov/geo/query/acc.cgi?acc=GSE152754).

The DESeq2 package (Love et al., 2014) was used to analyze the differential gene expression between the groups. The differentially expressed genes (DEGs) were identified as the fold changes of the expression levels greater than 2 and with a *p*-value of less than 0.1. The Database for Annotation, Visualization and Integrated Discovery (DAVID) (Huang et al., 2009) and gene ontology (GO) resource (The gene Ontology Consortium, 2019) were used to perform enrichment analysis on the DEGs. The protein–protein interaction (PPI) was analyzed using the STRING database (Szklarczyk et al., 2019) and visualized with Cytoscape (Shannon et al., 2003). Hub genes were identified using cytoHubba (Chin et al., 2014).

2.10. Statistical analysis

R software (version 3.6.1) (R Core Team, 2020) was used to perform the statistical analysis. Differences in body weight, sucrose preference, and OFT test results were analyzed by the one-way analysis of variance (ANOVA), followed by Dunnett's test of multiple comparisons with a control. Tukey's Honest Significant Difference (HSD) test was used to identify significant differences among groups for serum concentrations of CRH, ACTH, CORT, E2, FSH, LH, and AMH. ROS levels and apoptosis of the oocytes were analyzed by the Kruskal–Wallis test followed by Dunn's test of multiple comparisons using rank sums. Fisher's exact test was used to analyze the mitochondrial distribution. Data were expressed as the mean ± SEM and a *p*-value of less than 0.05 was considered statistically significant.

3. Results

3.1. Chemical components of KYZY

Twelve chemical components were identified in the KYZY by UPLC/HRMS. In the positive mass chromatogram, five components were identified: arginine (observed *m/z*: 173.1038, RT: 0.72 min); paeonol (observed *m/z*: 167.0726, RT: 13.48 min); atractylenolide III (observed *m/z*: 247.1349, RT: 17.20 min); ligustilide (observed *m/z*: 191.1079, RT: 18.59 min); atractylenolide I (observed *m/z*: 231.1384, RT: 20.44 min). In the negative mass chromatogram, another seven components were identified: citrulline (observed *m/z*: 174.0878, RT: 0.77 min); gallic acid (observed *m/z*: 169.0149 and 191.0214, RT: 1.71 min); tryptophan (observed *m/z*: 203.0832, RT: 3.89 min); oxypaeoniflora (observed *m/z*: 495.1521 and 541.1520, RT: 4.84 min); paeoniflorin (observed *m/z*: 479.1569 and 525.1602, RT: 5.39 min); galloylpaeoniflorin (observed *m/z*: 631.1686, RT: 6.18 min); mudanpioside J (observed *m/z*: 629.1911, RT: 8.73 min) (Fig. 1, Table 1, and Supplementary Fig. S1).

3.2. Mouse body weight and behaviors

CUSM was first assessed by body weight gain, the sucrose preference test, and an open-field test. The mice in the three KYZY groups had not yet been treated with the KYZY decoction at this stage. Thus, we also referred to the KYZY groups as the stressed groups in this section and the next section (3.2 and 3.3).

The animals under stress gained significantly lower body weight than the control group (Fig. 2A). From day 14, the mice in the stressed groups weighted significantly lower than the controls ($p < 0.001$).

The sucrose preference test showed that the stressed groups had a significantly reduced sucrose intake compared to the controls without stress (Fig. 2B, $p < 0.01$), suggesting that the stress caused anhedonia, which is a typical symptom of depression.

Mouse behaviors were further analyzed using the open-field test. The stressed groups spent significantly more time at rest than the control group (Fig. 2C, $p < 0.01$). Consistently, the moving time and total distance travelled as indicators of locomotor activity were significantly reduced in the stressed groups (Fig. 2D and E, $p < 0.01$). Further analysis of exploratory behavior found that the stressed mice spent significantly less time in the center zone, and significantly more time in the peripheral zone compared to the controls (Fig. 2F and G, $p < 0.01$). This finding suggests that the stress caused fear and anxiety in the mice (Himanshu et al., 2020).

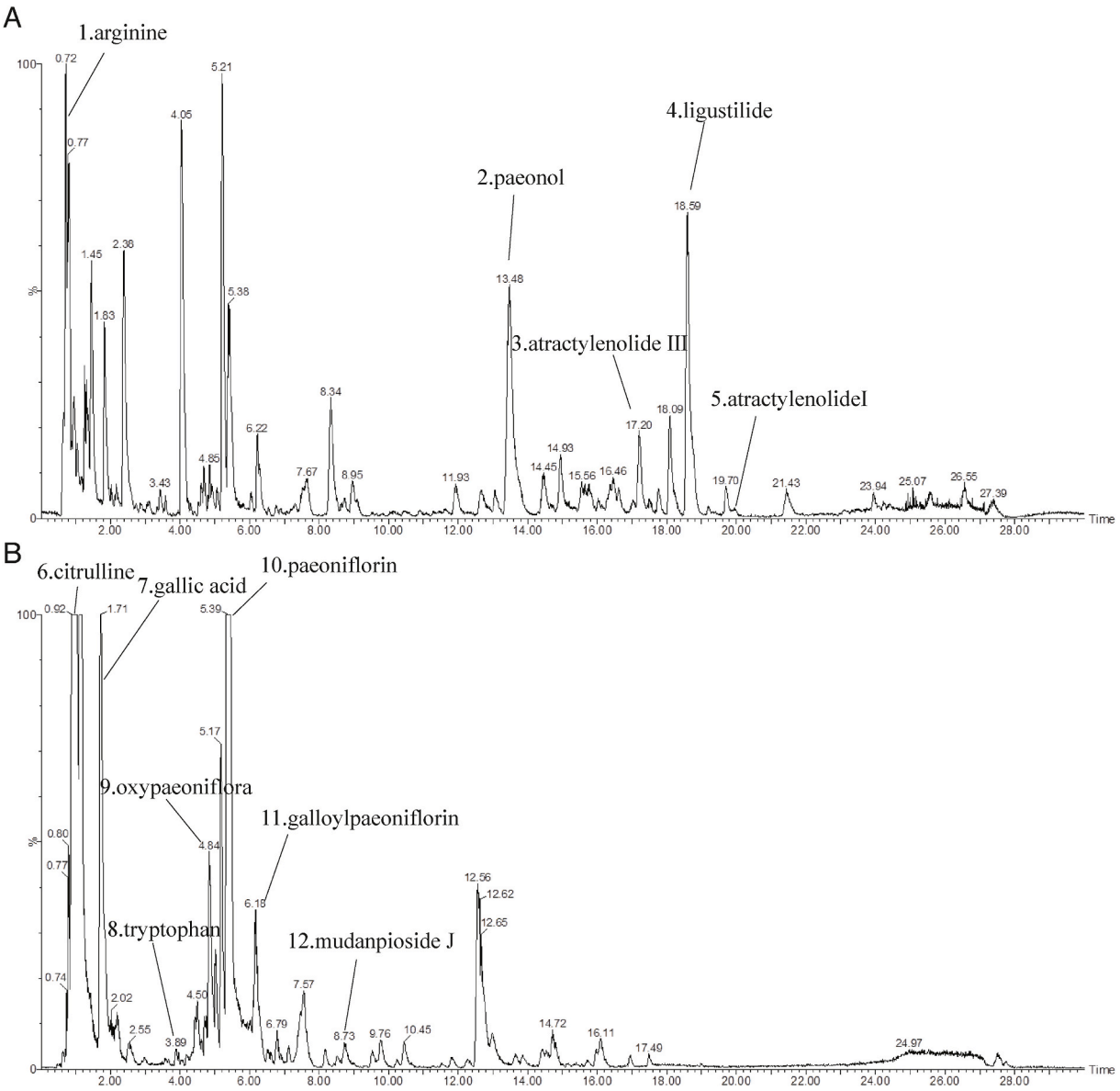

Fig. 1. Analysis of chemical components in KYZY. Twelve components were identified in the KYZY by UPLC/HRMS. (A) In the [M+H]+ model, five components were identified: 1. arginine; 2. paeonol; 3. atractylenolide III; 4. ligustilide; 5. atractylenolide I. (B) In the [M–H]– model, seven components were identified: 6. citrulline; 7. gallic acid; 8. tryptophan; 9. oxypaeoniflora; 10. paeoniflorin; 11. galloylpaeoniflorin; 12. mudanpioside J.

Table 1
Chemical components in KYZY.

Peak number	Compounds	Molecular formula	KYZY			Standards		
			RT (min)	[M+H]+	[M-H]-	RT (min)	[M+H]+	[M-H]-
1	arginine	C6H14N4O2	0.72	173.1038	–	0.67	173.1065	
2	paeonol	C9H10O3	13.48	167.0726	–	13.30	167.0687	–
3	atractylenolide III	C15H20O3	17.20	247.1349	–	17.15	247.1354	–
4	ligustilide	C12H14O2	18.59	191.1079	–	18.56	191.1072	–
5	atractylenolide I	C15H18O2	20.44	231.1384	–	20.46	231.1356	–
6	citrulline	C6H13N3O3	0.77	–	174.0878	0.73	–	174.0905
7	gallic acid	C30H32O15	1.71	–	169.0149, 191.0214	1.71	–	170.0215
8	tryptophan	C11H12N2O2	3.89	–	203.0832	3.89		203.0817
9	oxypaeoniflora	C23H28O12	4.84	–	495.1521, 541.1520	4.43	–	495.1572
10	paeoniflorin	C23H28O11	5.39	–	479.1569, 525.1602	5.35	–	479.1586
11	galloylpaeoniflorin	C30H32O15	6.18	–	631.1686	6.16	–	631.1658
12	mudanpioside J	C31H34O14	8.73	–	629.1911	8.98	–	629.1882

Peak numbers 1–5 and 6–12 were from positive and negative mass chromatogram, respectively.

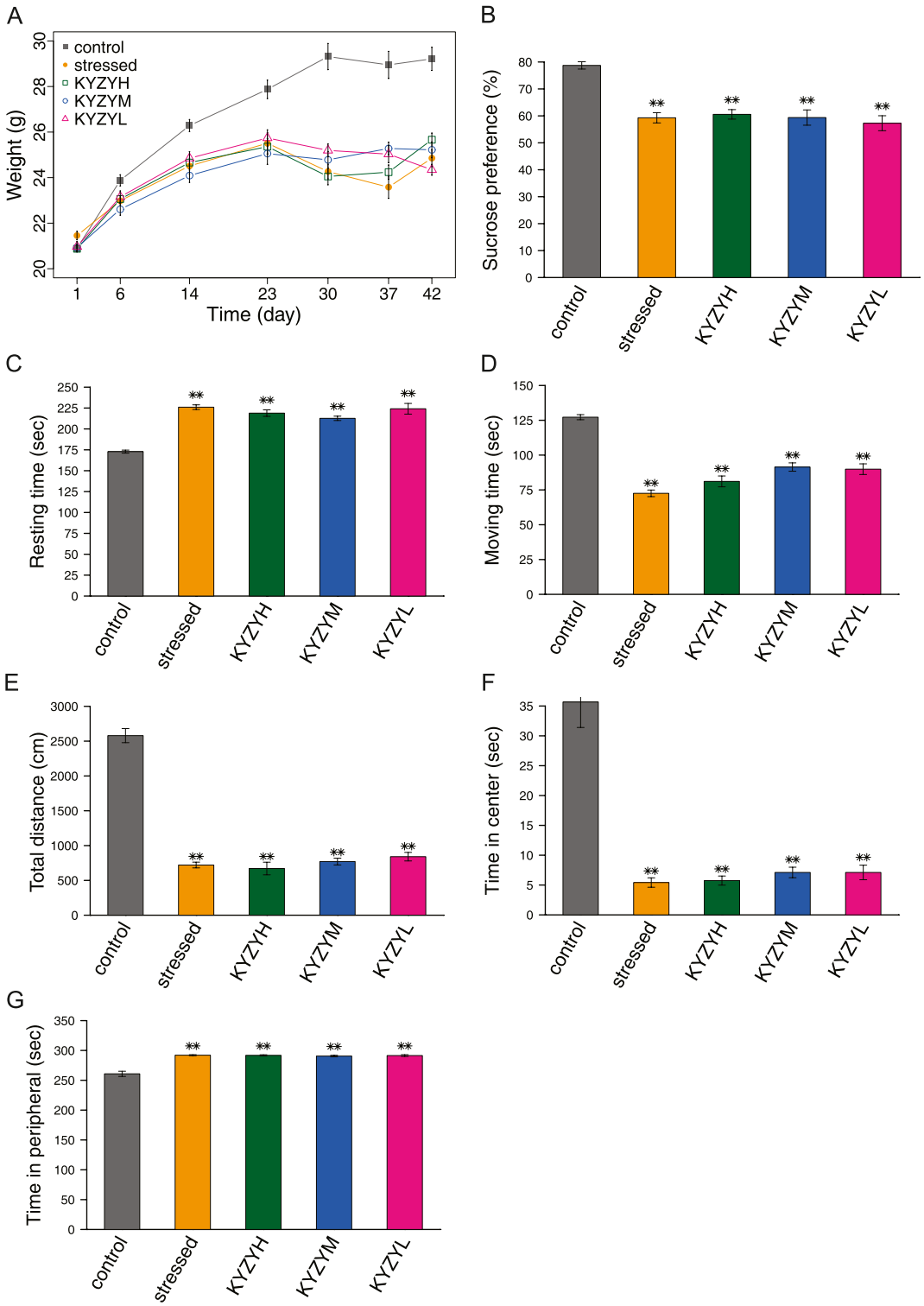

Fig. 2. Changes of mouse weight and behaviors. Mice were treated with stress for 6 weeks in the following groups: CUSM, high dose (KYZYH), medium dose (KYZYM), and low dose (KYZYL) of KYZY. Mice were not treated in the control group. The mice in the three KYZY groups had not yet been treated with the KYZY decoction at this stage. Mice were weighed on the days indicated (A, n = 30 in each group). Sucrose preference test (B) and open-field test for the resting time (C), moving time (D), total distance travelled in 5 min (E), time spent in the center zone (F), and time spent in the peripheral zone (G) were performed after completion of the CUSM. Data were expressed as the mean ± SEM. $^{**}p < 0.01$ by Dunnett's test for the differences between the stressed or KYZY groups and the control group.

3.3. Changes of HPA axis hormones

The mice in the stressed groups had significantly increased CRH, ACTH, and CORT serum levels compared to the controls (Fig. 3A, B, and C, $p < 0.01$). These results are consistent with the positive effect of stress on the HPA axis, stemming from the hypothalamus that secretes CRH to the adrenal cortex that releases CORT. The mice had not yet been treated with the decoction in the KYZY group at this stage.

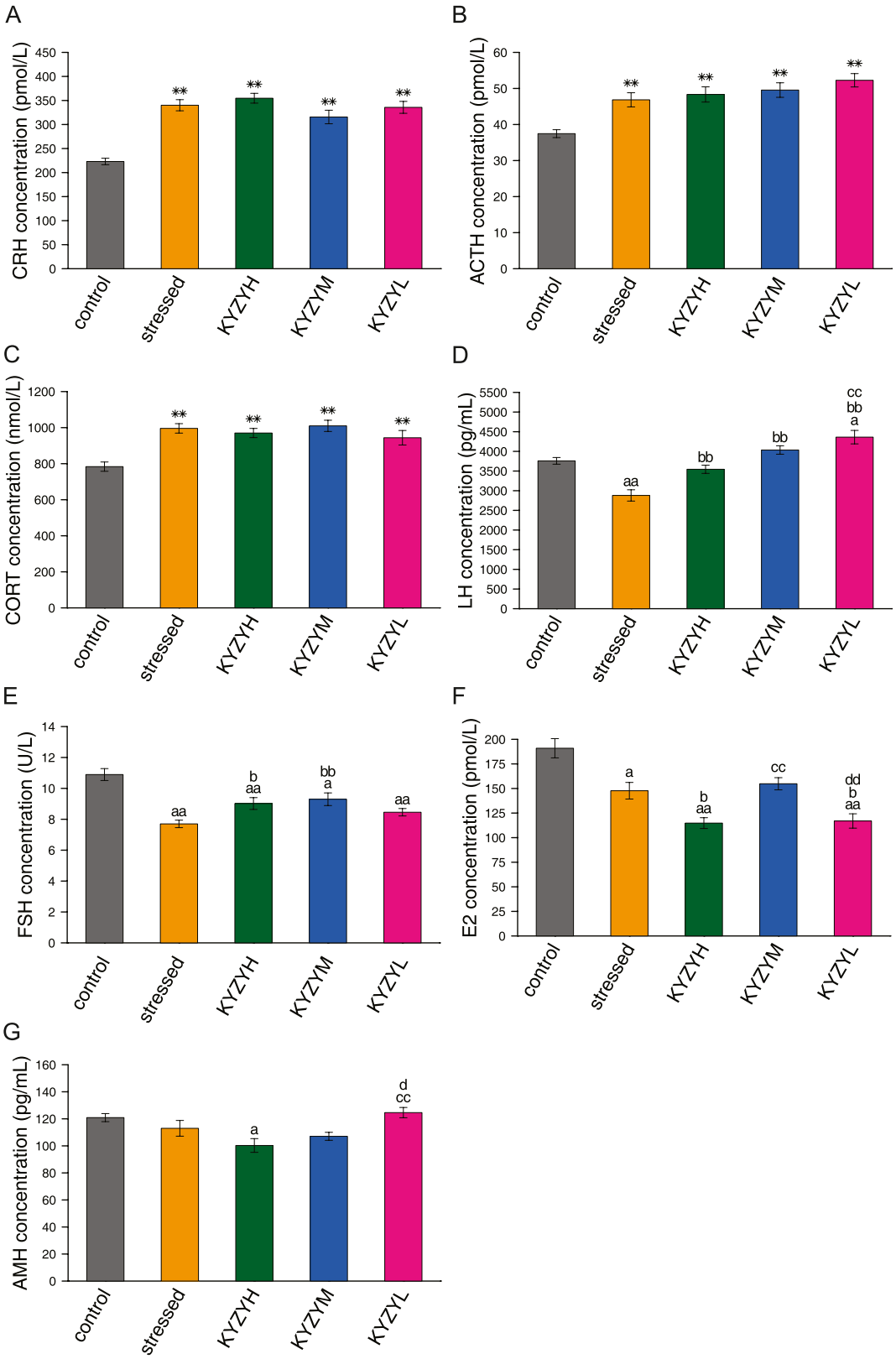

Fig. 3. Changes of serum hormonal levels. Serum levels of CRH (A), ACTH (B), CORT (C), LH (D), FSH (E), E2 (F), and AMH (G) were measured by ELISA. Data were expressed as the mean ± SEM. $^{**}p < 0.01$ by Dunnett's test for the differences between the stressed or KYZY groups and the control group (CRH, ACTH, and CORT). Differences among groups were analyzed by ANOVA followed by *post hoc* multiple comparisons using Tukey's HSD test (LH and FSH), or Kruskal-Wallis rank sum test followed by Dunn's test of multiple comparisons (E2 and AMH). a: $p < 0.05$ or aa: $p < 0.01$, compared to the control. b: $p < 0.05$ or bb: $p < 0.01$, compared to the stressed group. cc: $p < 0.01$, compared to the KYZYH group. d: $p < 0.05$ or dd: $p < 0.01$, compared to the KYZYM group. Measurement of the serum levels of CRH, ACTH, and CORT was done before the mice were treated with KYZY. For the LH, FSH, E2, and AMH, the measurement was done after the mice were treated with KYZY.

3.4. Changes of serum ovarian hormones

The LH, FSH, and E2 serum levels were significantly reduced in the stressed group compared to the controls (Fig. 3D, E, and F, $p < 0.05$). A medium dose of the KYZY treatment reversed the LH and FSH levels, and thus, they were significantly higher than the stressed group ($p < 0.01$). The levels of LH and E2 were not significantly different from the controls ($p > 0.05$). The serum levels of AMH did not change in either the stressed group or the KYZYM group ($p > 0.05$). AMH plays an important role in regulating the ovarian reserve (Victoria et al., 2019). Thus, our results suggested that stress and a medium dose of the KYZY treatment did not significantly impact the ovarian reserve. However, a high dose of KYZY significantly reduced the AMH levels compared to the controls ($p < 0.05$).

3.5. ROS levels in oocytes

The ROS levels in the oocytes were measured using DCFH-DA (Wang et al., 2013), which is permeable to the cell membrane and is hydrolyzed by cellular esterases to form a membrane-impermeable and active form of 2′,7′-dichlorodihydrofluorescein. ROS oxidize the latter molecule to produce 2′,7′-dichlorofluorescein, which is fluorescent. Therefore, the

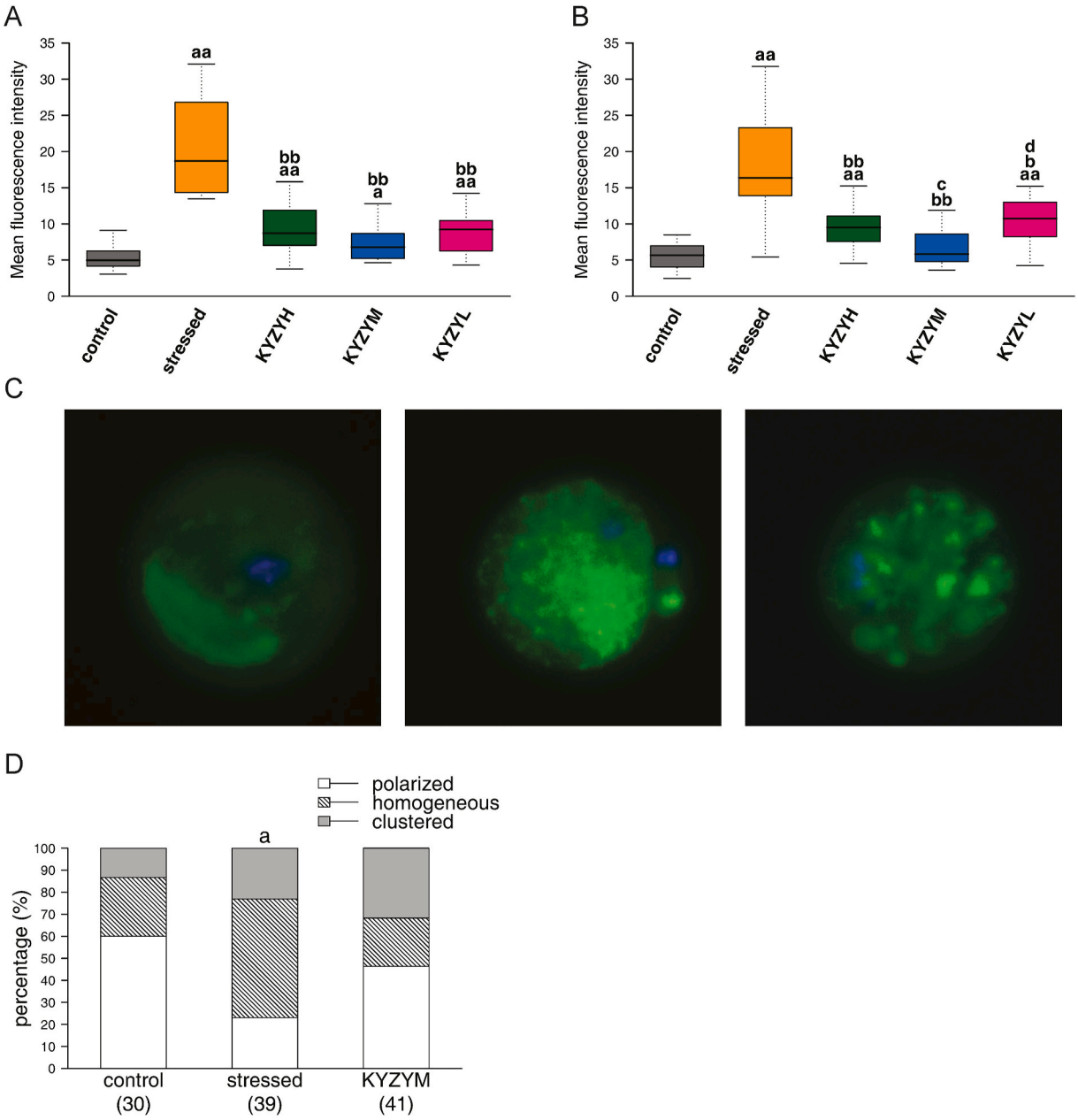

Fig. 4. Analysis of the ROS levels, apoptosis and mitochondria distribution in the oocytes. The isolated oocytes were stained with DCFH-DA to quantify the ROS levels (A) or TUNEL assay kit to assess apoptosis (B) or Mito-Tracker Green to image the mitochondrial distribution (C and D). The number of the oocytes is indicated in the parenthesis in D. The differences between groups for the ROS levels and apoptosis were analyzed by Dunn's test of multiple comparisons using rank sums. a: $p < 0.05$ or aa: $p < 0.01$, compared to the control. b: $p < 0.05$ or bb: $p < 0.01$, compared to the stressed group. c: $p < 0.05$, compared to the KYZYH group. d: $p < 0.05$, compared to the KYZYM group. Figure C showed the oocytes with polarized (left), homogeneous (middle), and clustered (right) distribution of mitochondria. The differences in the mitochondrial distribution were tested using Fisher's exact test. a: $p < 0.05$ between the stressed group and the control, and between the medium dose of KYZY-treated group and the stressed group. (For interpretation of the references to color in this figure legend, the reader is referred to the Web version of this article.)

intracellular ROS levels can be analyzed by measuring the fluorescent intensity of the metabolized and oxidized product of DCFH-DA. The stressed group had significantly higher ROS levels than the control group (Fig. 4A, $p < 0.01$). All three KYZY treatments reversed the ROS levels, which rendered them significantly different from the stressed group ($p < 0.01$), suggesting an antioxidant effect.

3.6. Oocyte apoptosis

DNA is hydrolyzed by a specific DNase that is activated during apoptosis. We analyzed the DNA fragmentation in oocytes using the TUNEL assay, which quantitatively detects the number of blunt ends from double-stranded DNA breaks (Kyrylkova et al., 2012). As measured by the fluorescent intensity, the number of apoptotic oocytes from the stressed group was significantly higher than the controls (Fig. 4B, $p < 0.01$). Similar to the ROS result, all three KYZY treatments reversed

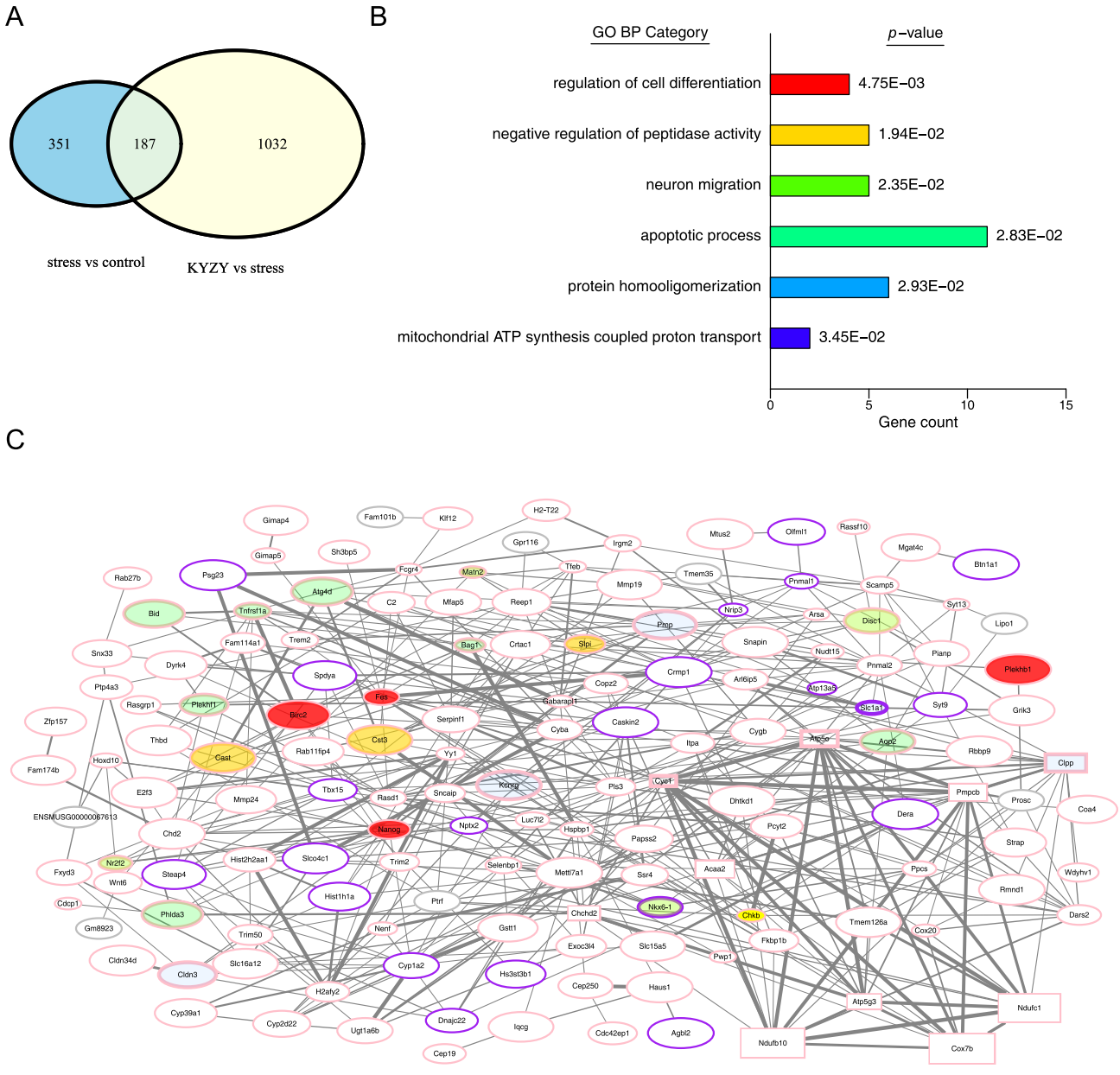

Fig. 5. Analysis of the DEGs. A is the Venn diagram showing the number of DEGs. There were 192 genes up-regulated and 346 down-regulated by the stress in the stress vs. control DEG set. There were 1092 genes up-regulated and 127 down-regulated by the medium dose of KYZY treatment in the KYZY vs. stress DEG set. In the common 187 DEGs, there were 31 genes first up-regulated by the stress and then down-regulated by the KYZY. The other 156 genes were first down-regulated by the stress and then up-regulated by the KYZY. B is gene enrichment analysis for the GO BP terms. X-axis is the number of DEGs identified in the GO-BP. *P*-value is the modified *p*-value from the Fisher's exact test. C is the protein–protein interaction network based on the 187 common DEGs. Rectangle nodes represent top 10 hub genes. Node fill color represents the GO BPs identified in the enrichment analysis (B). Node border color represents differential gene expression with pink for down-regulation and violet up-regulation in the stressed oocytes compared to the controls. Thickness of the edge connecting nodes represents the confidence levels of the interaction computed as the combined scores from the STRING database, with thicker edges for higher confidence. The size of the nodes represents the *p*-value in the result of the DESeq analysis, which indicates the probability that a fold change is likely or more likely under the null hypothesis of no difference, with larger sizes more likely having the differential expression. (For interpretation of the references to color in this figure legend, the reader is referred to the Web version of this article.)

apoptosis to the extent that it was significantly different from the stressed group ($p < 0.05$), suggesting an anti-apoptotic effect.

3.7. Mitochondrial distribution in oocytes

The Mito-Tracker Green staining showed that 60% of the mitochondria were in a polarized distribution in the oocytes of the control group (Fig. 4C and D). Stress significantly changed the mitochondria distribution ($p < 0.01$). The polarized distribution reduced to 23%, and the homogenous distribution and the clustered distribution increased to 54% and 23%, respectively. A medium dose of the KYZY treatment reversed the mitochondria distribution in a manner that was not significantly different from that of the control ($p > 0.05$). The polarized distribution increased to 46%, which was significantly different from that of the stressed group ($p < 0.05$), but not from the controls ($p > 0.05$). Accordingly, the homogeneous distribution reduced to 22%, and the clustered distribution increased to 32%.

3.8. DEG analysis

We identified 538 DEGs between the stressed and control groups, and 1219 DEGs between the medium dose KYZY-treated and the stressed groups. There were 187 genes common to both sets of DEGs (Fig. 5A). Among these genes, 31 were up-regulated by stress and down-regulated by the KYZY treatment. The other 156 genes were down-regulated by stress and up-regulated by the KYZY treatment.

A functional enrichment analysis identified 6 gene ontology (GO) biological process (BP) terms that were significantly enriched in the 187 common DEGs (Fig. 5B and Table 2). The GO BP "apoptotic process" had the most genes (11), suggesting that its regulation by the stress and the KYZY was important in the oocytes.

A PPI network was constructed using the 187 DEGs regulated by both the stress and the KYZY (Fig. 5C). A network analysis further identified the top 10 hub genes that were the most important nodes (Table 3). These are often central regulatory elements in the biological pathways (Chin et al., 2014). All of the top 5 hub genes were components of the mitochondrial respiratory chain or ATP synthase, suggesting that they are central to the stress response and might be possible targets of the KYZY.

4. Discussion

Psychological stress affects female reproductive function. Although the causal relationship between stress and infertility in humans is still unclear, stress reduction can increase pregnancy success (Lovely et al., 2003; Rooney and Domar, 2018). Stress induces changes in the levels of hormones associated with the HPA and HPO axes, which in turn affect oocyte quality, fertilization, and embryo development (An et al., 2013; Prasad et al., 2016). Furthermore, the HPA axis has direct inhibitory effect on the HPO (Valsamakis et al., 2019).

KYZY is a classic recipe in TCM that has been used to treat infertility for more than 300 years (Fu, 2006). To characterize the effects of KYZY, we first subjected the decoction to UPLC/HRMS, which identified twelve components: arginine, paeonol, atractylenolide III, ligustilide, atractylenolide I, citrulline, gallic acid, tryptophan, oxypaeoniflora, paeoniflorin, galloylpaeoniflorin, and mudanpioside J. Many of these components have implications in depression and neural cell health. The detection of arginine and citrulline aligns with reports that the arginine metabolic pathway is associated with depression (Ozden et al., 2020). In addition, the amino acid tryptophan is the precursor of serotonin, a neurotransmitter involved in depression (Yohn et al., 2017). Moreover, individual administration of paeoniflorin (Liu et al., 2019), paeonol (Tao et al., 2016), atractylenolide I (Gao et al., 2018), and gallic acid (Salehi et al., 2018; Samad et al., 2019) in a murine model of depression (Liu et al., 2019) was effective in ameliorating depressive symptoms.

Table 2
Genes in the enriched GO biological processes.

GO term	Genes
mitochondrial ATP synthesis coupled proton transport	*Cyc1*, *Atp5o*
protein homooligomerization	*Bid*, *Kcnrg*, *Slc1a1*, *Clpp*, *Cldn3*, *Prnp*
apoptotic process	*Aqp2*, *Birc2*, *Bag1*, *Lgals7*, *Bid*, *Cst3*, *Atg4d*, *Wt1*, *Plekhf1*, *Phlda3*, *Tnfrsf1a*
neuron migration	*Disc1*, *Matn2*, *Nkx6-1*, *Pex2*, *Nr2f2*
negative regulation of peptidase activity	*Cst3*, *Cast*, *Serpina3n*, *Slpi*, *Pzp*
regulation of cell differentiation	*Plekhb1*, *Birc2*, *Fes*, *Nanog*

DEGs were used to query the GO database for enrichment of biological process (BP). Six GO BP terms were identified ($p < 0.05$). All the genes were down-regulated in the CUSM group, but up-regulated by a medium dose of KYZY treatment except *Slc1a1*, *Nkx6-1*, and *Pzp*. The latter three genes were up-regulated in the CUSM group, but down-regulated by the KYZY treatment.

Table 3
Hub genes identified in the protein interaction network.

Genes	Full name and function	MCC score
Atp5o	ATP synthase peripheral stalk subunit OSCP It functions in ATP synthesis, as part of the connector linking the F1 catalytic core and the F0 membrane proton channel of the ATP synthase.	2738
Ndufb10	NADH:ubiquinone oxidoreductase subunit B10 It is an accessory subunit of Complex I which transfer electrons from NADH to ubiquinone	2666
Cyc1	cytochrome c-1 It is the catalytic core subunit of Complex III that transfers electrons from ubiquinone to cytochrome C.	2585
Atp5g3	ATP synthase, H+ transporting, mitochondrial F0 complex, subunit C3 (subunit 9) It functions in ATP synthesis, as part of the ATP synthase complex F_0 domain's c-ring.	2307
Cox7b	cytochrome c oxidase subunit 7B It is a component of cytochrome c oxidase (Complex IV) which catalyzes the reduction of oxygen to water with the electrons transferred from the reduced cytochrome C	2185
Pmpcb	peptidase (mitochondrial processing) beta It is the catalytic subunit of the essential mitochondrial processing protease which is responsible for the maturation of the majority of mitochondria precursor proteins (Jadiya and Tomar, 2020). Defects in Pmpcb resulted in defective biosynthesis of the iron-sufur cluster of the respiratory chain (Vogtle et al., 2018).	1977
Ndufc1	NADH:ubiquinone oxidoreductase subunit C1 It is an accessory subunit of Complex I which transfer electrons from NADH to ubiquinone	1705
Acaa2	acetyl-Coenzyme A acyltransferase 2 (mitochondrial 3-oxoacyl-Coenzyme A thiolase) It functions in the last step of β-oxidation pathway which breaks down fatty acids into acetyl-CoA	976
Chchd2	coiled-coil-helix-coiled-coil-helix domain containing 2 It functions as a transcription factor in nuclei and regulate the expression of the subunit 4 isoform 2 of cytochrome C oxidase and *Chchd2* itself under oxidative or hypoxic stress (Zhou et al., 2020). In mitochondria, it is required for the activity of respiratory chain and is a negative regulator of mitochondria-mediated apoptosis	753
Clpp	caseinolytic mitochondrial matrix peptidase proteolytic subunit It is a mitochondrial serine protease and has a housekeeping role for cleavage of defective respiratory chain proteins and maintaining the integrity of the mitochondrial respiratory chain (Mirali and Schimmer, 2020)	313

Top ten hub genes were identified using CytoHubba (Chin et al., 2014b) and ranked by the Maximal Clique Centrality (MCC) scores. The official full names were from the Gene database of National Center for Biotechnology Information (NCBI) (https://www.ncbi.nlm.nih.gov/gene). The function descriptions were from NCBI and the Universal Protein Resource (UniProt, https://www.uniprot.org) with additional referenced information as indicated.

Meanwhile, atractylenolide III has been observed to prevent corticosterone-induced neuronal cell death (Gong, W.X. et al., 2019). Finally, antioxidant and anti-inflammatory activities have been reported for some of these compounds, such as galloylpaeoniflorin (Wen et al., 2018), paeoniflorin, and oxypaeoniflora (Zhang et al., 2013). Therefore, the effectiveness of KYZY in treating infertility is likely due at least in part to the antidepressant, antioxidant, and anti-inflammatory activities of its major constituents.

Stress is documented to elevate serum levels of CRH, ACTH, and CORT, and furthermore to reduce serum levels of LH, E2, and FSH, suggesting inhibition of the HPO axis by the HPA axis (Valsamakis et al., 2019). A medium dose of KYZY was found to restore LH and E2 to their normal control levels, suggesting that it might target some aspects of the HPA and/or HPO axis; this is consistent with results observed with other antidepressant herbal recipes that caused decreases in the levels of HPA axis hormones (Zhang et al., 2019).

In the context of pregnancy, serum levels of AMH are important for being correlated with the ovarian reserve (Barranco et al., 2020). Prolonged stress can induce reduction in the ovarian reserve and so decrease serum AMH (Gao et al., 2020). However, we did not observe any significant change in serum AMH following stress in the CUSM group. This discrepancy was probably due to differences in stress duration and/or the mouse strain used. In terms of KYZY treatment, a high dose appeared to reduce AMH levels while a low dose significantly increased AMH levels.

Another key indicator is ROS, which at physiological levels act as secondary messengers and are essential for oocyte maturation, ovulation, fertilization, and early embryo development (Shkolnik et al., 2011; von Mengden et al., 2020). However, increased metabolism at these stages leads to active ROS production and, together with decreased antioxidant capacity, makes oocytes and early embryos prone to oxidative stress (OS) (Agarwal et al., 2012; Prasad et al., 2016). Stress then induces elevated levels of ROS in oocytes and impairs oocyte quality through disrupting spindle assembly, with subsequent chromatin misalignment (Gao et al., 2016; Guo et al., 2020; Prasad et al., 2016; Zhou et al., 2012). We showed that ROS levels in oocytes from the CUSM group were significantly increased compared to the control group. KYZY treatment reduced ROS levels, consistent with the antioxidant activities of some of its components. Thus, KYZY might improve oocyte quality by reducing ROS levels.

Mitochondria are the major organelles that generate ROS and are prone to OS (Agarwal et al., 2012). Furthermore, OS contributes to decline of oocyte quality and depletion of the ovarian reserve by inducing apoptosis (Agarwal et al., 2005; Lu et al., 2018; Prasad et al., 2016). Using the TUNEL assay to detect apoptotic DNA fragments in oocytes, we observed increased apoptosis in the CUSM group compared to the control group. We found that KYZY treatment reduced this apoptosis, suggesting a protective effect; this may also be attributable to the antioxidant components of KYZY.

Beyond ROS, oocyte maturation, fertilization and embryo development depend on the polarized distribution and multiple other functions of mitochondria, including energy production, calcium balancing, and redox maintenance (Roth, 2018). Notably, a dynamic change in mitochondria distribution occurs during oocyte maturation. During meiotic division, mitochondria aggregate around the spindle to provide energy for the extrusion of the polar body (Babayev and Seli, 2015; Lei et al., 2014; Ou et al., 2012). Their polarized distribution is a sign of cytoplasmic maturation and ensures the correct separation of chromosomes (Sun and Schatten, 2006). Thus, OS also acts to reduce oocyte quality by impairing mitochondrial function and increasing aneuploidy (Sasaki et al., 2019; Sharma et al., 2013; Slozina and Neronova, 1990; Zhou et al., 2012). Consistent with these reports, we found that stress reduced the polarized distribution of mitochondria in the CUSM group, while KYZY treatment ameliorated that abnormal distribution.

RNAseq of the stressed and treated groups identified DEGs that were enriched in six GO BP terms. Of the 33 genes representing those terms, 11 were annotated with “apoptotic process”, suggesting that apoptosis is a major pathway activated by stress. This aligns with the results of our TUNEL assay, which revealed increased apoptotic oocytes in the CUSM group and reduction of that apoptosis by KYZY treatment.

Two other genes, cytochrome c-1 (*Cyc1*) and ATP synthase O subunit (*Atp5o*), were associated with the GO BP term “mitochondrial ATP synthesis coupled proton transport”. These are essential to the main function of mitochondria, which is ATP production via the ATP synthase in the mitochondrial inner membrane, driven by the proton gradient generated by the mitochondrial respiratory chain: CYC1 is the catalytic core subunit of complex III of the respiratory chain, while ATP5O is part of the ATP synthase F_0 domain and the peripheric stalk. Expression of both genes was down-regulated by stress and up-regulated by KYZY treatment, suggesting that they are molecular targets of KYZY.

Both CYC1 and ATP5O were among the top ten hub proteins in the PPI network. The other eight such proteins are also localized to the mitochondria, and are either components of one of the four complexes of the respiratory chain (NDUFB10, COX7B, NDUFC1) or ATP synthase (ATP5G3) or regulate the function of the respiratory chain (PMPCB, ACAA2, CHCHD2, CLPP) (Table 3). This suggests that the respiratory chain/ATP production is the key target of stress, and KYZY can ameliorate the negative effects of stress either directly by acting on the complexes of the respiratory chain or indirectly through the greater associated PPI network. The reason as to why only *Atp5o* and *Cyc1* were identified in the “mitochondrial ATP synthesis coupled proton transport” GO BP is likely due to their indispensable roles in the respiratory chain.

Most DEGs among the six enriched GO BPs were down-regulated by stress, but up-regulated by KYZY treatment. Three exceptions were up-regulated by stress, but down-regulated by KYZY treatment: *Slc1a1*, *Pzp*, and *Nkx6-1*.

SLC1A1 is a member of the sodium-dependent glutamate transporter family, which mediates glutamate and cysteine uptake into the cell for glutathione (GSH) synthesis and to control extracellular glutamate levels (Aoyama and Nakaki, 2015; Suarez-Pozos et al., 2020). Importantly, GSH functions as an antioxidant and is the major regulator of intracellular redox status; thus, elevated expression of *Slc1a1* in the CUSM group likely reflected the need to synthesize more GSH to counter OS.

PZP, also known as A2M, is a broad-spectrum plasma protease inhibitor (Rehman et al., 2013). An early study reported it to inhibit mouse embryo development *in vitro* (Sayegh et al., 1997). More recently, PZP has been demonstrated important in maintaining homeostasis during dietary restriction due to its ability to trap and inhibit various proteinases released from damaged cells (Schelp et al., 2019); furthermore, it can be activated by OS and, due to its increased surface hydrophobicity, functions as a chaperone to prevent aggregation of disease-associated proteins (Dahl et al., 2015). Thus, PZP is likely protective for oocytes under stress.

NKX6-1 was discovered as an important transcription factor in endocrine progenitor cells (Sander et al., 2000) and is required for the generation of insulin-producing β cells (Schaffer et al., 2013). Downstream target genes of NKX6-1 are the α-cell determinant *Arx*, nuclear receptors *Nr4a1* and *Nr4a3*, and cell cycle regulators including E2F transcription factor 1, cyclin E1, and components of the anaphase-promoting complex. Administration of glucocorticoids is associated with neogenesis of β-cells in mice (Russell and Leete, 2019), suggesting that the expression of *NKX6-1* could be regulated by stress; namely, the stress-induced up-regulation of *Nkx6-1* in our study could be mediated by increased levels of glucocorticoids. However, the exact function of NKX6-1 in oocytes remains unclear.

5. Conclusion

Our study supports the antioxidant and anti-apoptosis effects of KYZY on oocytes. KYZY also ameliorated the adverse effects of stress on

ovarian hormones and mitochondrial function in oocytes. The transcriptomic analysis suggests that stress regulates oocyte mitochondrial electron transport and ATP synthesis, and KYZY may target the mitochondrial respiratory chain and ATP synthase.

Authors' contributions

Tian Xia and Ruihong Ma had the initial idea, designed the research, and acquired the funding. Xiaoli Zhao performed the experiments including data collection and analysis, and drafted the manuscript. Xiaoyu Zhang provided important assistance for the experiments. Baojuan Wang supervised the whole project. Beilei Rong, Nan Jiang, Weihua Feng, and MingLi Chen were involved in the animal experiments. Zhipeng Huo and Shuming Li performed the UPLC/HRMS analysis of KYZY. All authors have read and approved the final manuscript.

Grant support

This work was supported by the National Natural Science Foundation of China (81603650).

Declaration of competing interest

The authors declare no conflicts of interest.

Appendix A. Supplementary data

Supplementary data to this article can be found online at https://doi.org/10.1016/j.jep.2021.114298.

References

Agarwal, A., Gupta, S., Sharma, R.K., 2005. Role of oxidative stress in female reproduction. Reprod. Biol. Endocrinol. 3, 28–48.
Agarwal, A., Aponte-Mellado, A., Premkumar, B.J., Shaman, A., Gupta, S., 2012. The effects of oxidative stress on female reproduction: a review. Reprod. Biol. Endocrinol. 10, 49–79.
An, Y., Sun, Z., Li, L., Zhang, Y., Ji, H., 2013. Relationship between psychological stress and reproductive outcome in women undergoing in vitro fertilization treatment: psychological and neurohormonal assessment. J. Assist. Reprod. Genet. 30 (1), 35–41.
Aoyama, K., Nakaki, T., 2015. Glutathione in cellular redox homeostasis: association with the excitatory amino acid carrier 1 (EAAC1). Molecules 20 (5), 8742–8758.
Babayev, E., Seli, E., 2015. Oocyte mitochondrial function and reproduction. Curr. Opin. Obstet. Gynecol. 27 (3), 175–181.
Barranco, I., Fernandez-Fuertes, B., Padilla, L., Delgado-Bermudez, A., Tvarijonaviciute, A., Yeste, M., 2020. Seminal plasma anti-mullerian hormone: a potential AI-boar fertility biomarker? Biology 9 (4), 78–90.
Bioinformatics Group at the Babraham Institute, 2019. Trim galore. Accessed July 01, 2020. http://www.bioinformatics.babraham.ac.uk/projects/trim_galore/.
Bradley, J., Swann, K., 2019. Mitochondria and lipid metabolism in mammalian oocytes and early embryos. Int. J. Dev. Biol. 63 (3–4-5), 93–103.
Chang, X., Jia, H., Zhou, C., Zhang, H., Yu, M., Yang, J., Zou, Z., 2015. Role of Bai-Shao towards the antidepressant effect of Chaihu-Shu-Gan-San using metabonomics integrated with chemical fingerprinting. J Chromatogr B Analyt Technol Biomed Life Sci 1006, 16–29.
Chin, C.H., Chen, S.H., Wu, H.H., Ho, C.W., Ko, M.T., Lin, C.Y., 2014. cytoHubba: identifying hub objects and sub-networks from complex interactome. BMC Syst. Biol. 8 (Suppl. 4), S11–S17. Suppl 4.
Cong, H., Gao, Q., Luan, Y., Li, N., 2020. Clinical observation on the pregnancy outcome of patients with liver depression and kidney deficiency type in vitro fertilization and embryo transfer. Journal of Liaoning University of Traditional Chinese Medicine 22 (10), 5–8.
Dahl, J.U., Gray, M.J., Jakob, U., 2015. Protein quality control under oxidative stress conditions. J. Mol. Biol. 427 (7), 1549–1563.
Das, S., Chattopadhyay, R., Ghosh, S., Ghosh, S., Goswami, S.K., Chakravarty, B.N., Chaudhury, K., 2006. Reactive oxygen species level in follicular fluid–embryo quality marker in IVF? Hum. Reprod. 21 (9), 2403–2407.
Ebbesen, S.M., Zachariae, R., Mehlsen, M.Y., Thomsen, D., Hojgaard, A., Ottosen, L., Petersen, T., Ingerslev, H.J., 2009. Stressful life events are associated with a poor in-vitro fertilization (IVF) outcome: a prospective study. Hum. Reprod. 24 (9), 2173–2182.
Edgar, R., Domrachev, M., Lash, A.E., 2002. Gene Expression Omnibus: NCBI gene expression and hybridization array data repository. Nucleic Acids Res. 30 (1), 207–210.
Feng, D.D., Tang, T., Lin, X.P., Yang, Z.Y., Yang, S., Xia, Z.A., Wang, Y., Zheng, P., Wang, Y., Zhang, C.H., 2016. Nine traditional Chinese herbal formulas for the treatment of depression: an ethnopharmacology, phytochemistry, and pharmacology review. Neuropsychiatric Dis. Treat. 12, 2387–2402.
Fu, S., 2006. Fu Qingzhu's Obstetrics and Gynecology (Based on an, 1869 edition. Chongwen Publishing House). People's Medical Publishing House, Beijing.
Gao, X., Zheng, X., Li, Z., Zhou, Y., Sun, H., Zhang, L., Guo, X., Du, G., Qin, X., 2011. Metabonomic study on chronic unpredictable mild stress and intervention effects of Xiaoyaosan in rats using gas chromatography coupled with mass spectrometry. J. Ethnopharmacol. 137 (1), 690–699.
Gao, Y., Chen, F., Kong, Q.Q., Ning, S.F., Yuan, H.J., Lian, H.Y., Luo, M.J., Tan, J.H., 2016. Stresses on female mice impair oocyte developmental potential: effects of stress severity and duration on oocytes at the growing follicle stage. Reprod. Sci. 23 (9), 1148–1157.
Gao, H., Zhu, X., Xi, Y., Li, Q., Shen, Z., Yang, Y., 2018. Anti-depressant-like effect of atractylenolide I in a mouse model of depression induced by chronic unpredictable mild stress. Exp Ther Med 15 (2), 1574–1579.
Gao, L., Zhao, F., Zhang, Y., Wang, W., Cao, Q., 2020. Diminished ovarian reserve induced by chronic unpredictable stress in C57BL/6 mice. Gynecol. Endocrinol. 36 (1), 49–54.
Gong, W., Zhu, S., Chen, C., Yin, Q., Li, X., Du, G., Zhou, Y., Qin, X., 2019. The anti-depression effect of Angelicae sinensis Radix is related to the pharmacological activity of modulating the hematological anomalies. Front. Pharmacol. 10, 192–209.
Gong, W.X., Zhou, Y.Z., Qin, X.M., Du, G.H., 2019. Involvement of mitochondrial apoptotic pathway and MAPKs/NF-kappa B inflammatory pathway in the neuroprotective effect of atractylenolide III in corticosterone-induced PC12 cells. Chin. J. Nat. Med. 17 (4), 264–274.
Guo, Y., Sun, J., Bu, S., Li, B., Zhang, Q., Wang, Q., Lai, D., 2020. Melatonin protects against chronic stress-induced oxidative meiotic defects in mice MII oocytes by regulating SIRT1. Cell Cycle 19 (13), 1677–1695.
Himanshu, Dharmila, Sarkar, D., Nutan, 2020. A review of behavioral tests to evaluate different types of anxiety and anti-anxiety effects. Clin Psychopharmacol Neurosci 18 (3), 341–351.
Huang, D.W., Sherman, B.T., Lempicki, R.A., 2009. Systematic and integrative analysis of large gene lists using DAVID bioinformatics resources. Nat. Protoc. 4 (1), 44–57.
Jadiya, P., Tomar, D., 2020. Mitochondrial protein quality control mechanisms. Genes 11 (5), 563–585.
Jamil, M., Debbarh, H., Aboulmaouahib, S., Aniq Filali, O., Mounaji, K., Zarqaoui, M., Saadani, B., Louanjli, N., Cadi, R., 2020. Reactive oxygen species in reproduction: harmful, essential or both? Zygote 28 (4), 255–269.
Kiapekou, E., Zapanti, E., Mastorakos, G., Loutradis, D., 2010. Update on the role of ovarian corticotropin-releasing hormone. Ann. N. Y. Acad. Sci. 1205, 225–229.
Kim, D., Paggi, J.M., Park, C., Bennett, C., Salzberg, S.L., 2019. Graph-based genome alignment and genotyping with HISAT2 and HISAT-genotype. Nat. Biotechnol. 37 (8), 907–915.
Kovaka, S., Zimin, A.V., Pertea, G.M., Razaghi, R., Salzberg, S.L., Pertea, M., 2019. Transcriptome assembly from long-read RNA-seq alignments with StringTie2. Genome Biol. 20 (1), 278–290.
Kyrylkova, K., Kyryachenko, S., Leid, M., Kioussi, C., 2012. Detection of apoptosis by TUNEL assay. Methods Mol. Biol. 887, 41–47.
Lei, T., Guo, N., Tan, M.H., Li, Y.F., 2014. Effect of mouse oocyte vitrification on mitochondrial membrane potential and distribution. J Huazhong Univ Sci Technolog Med Sci 34 (1), 99–102.
Liu, M.Y., Yin, C.Y., Zhu, L.J., Zhu, X.H., Xu, C., Luo, C.X., Chen, H., Zhu, D.Y., Zhou, Q. G., 2018. Sucrose preference test for measurement of stress-induced anhedonia in mice. Nat. Protoc. 13 (7), 1686–1698.
Liu, S.C., Hu, W.Y., Zhang, W.Y., Yang, L., Li, Y., Xiao, Z.C., Zhang, M., He, Z.Y., 2019. Paeoniflorin attenuates impairment of spatial learning and hippocampal long-term potentiation in mice subjected to chronic unpredictable mild stress. Psychopharmacology (Berlin) 236 (9), 2823–2834.
Louis, G.M., Lum, K.J., Sundaram, R., Chen, Z., Kim, S., Lynch, C.D., Schisterman, E.F., Pyper, C., 2011. Stress reduces conception probabilities across the fertile window: evidence in support of relaxation. Fertil. Steril. 95 (7), 2184–2189.
Love, M.I., Huber, W., Anders, S., 2014. Moderated estimation of fold change and dispersion for RNA-seq data with DESeq2. Genome Biol. 15 (12), 550–570.
Lovely, L.P., Meyer, W.R., Ekstrom, R.D., Golden, R.N., 2003. Effect of stress on pregnancy outcome among women undergoing assisted reproduction procedures. South. Med. J. 96 (6), 548–551.
Lu, J., Wang, Z., Cao, J., Chen, Y., Dong, Y., 2018. A novel and compact review on the role of oxidative stress in female reproduction. Reprod. Biol. Endocrinol. 16 (1), 80.
Mirali, S., Schimmer, A.D., 2020. The role of mitochondrial proteases in leukemic cells and leukemic stem cells. Stem Cells Transl Med 9 (12), 1481–1487.
Nepomnaschy, P.A., Welch, K.B., McConnell, D.S., Low, B.S., Strassmann, B.I., England, B.G., 2006. Cortisol levels and very early pregnancy loss in humans. Proc. Natl. Acad. Sci. U. S. A. 103 (10), 3938–3942.
Ou, X.H., Li, S., Wang, Z.B., Li, M., Quan, S., Xing, F., Guo, L., Chao, S.B., Chen, Z., Liang, X.W., Hou, Y., Schatten, H., Sun, Q.Y., 2012. Maternal insulin resistance causes oxidative stress and mitochondrial dysfunction in mouse oocytes. Hum. Reprod. 27 (7), 2130–2145.
Ozden, A., Angelos, H., Feyza, A., Elizabeth, W., John, P., 2020. Altered plasma levels of arginine metabolites in depression. J. Psychiatr. Res. 120, 21–28.
Peters, A.E., Mihalas, B.P., Bromfield, E.G., Roman, S.D., Nixon, B., Sutherland, J.M., 2020. Autophagy in female fertility: a role in oxidative stress and aging. Antioxidants Redox Signal. 32 (8), 550–568.

Picelli, S., Björklund Å, K., Faridani, O.R., Sagasser, S., Winberg, G., Sandberg, R., 2013. Smart-seq2 for sensitive full-length transcriptome profiling in single cells. Nat. Methods 10 (11), 1096–1098.
Prasad, S., Tiwari, M., Pandey, A.N., Shrivastav, T.G., Chaube, S.K., 2016. Impact of stress on oocyte quality and reproductive outcome. J. Biomed. Sci. 23, 36–40.
Puscheck, E.E., Bolnick, A., Awonuga, A., Yang, Y., Abdulhasan, M., Li, Q., Secor, E., Louden, E., Huttemann, M., Rappolee, D.A., 2018. Why AMPK agonists not known to be stressors may surprisingly contribute to miscarriage or hinder IVF/ART. J. Assist. Reprod. Genet. 35 (8), 1359–1366.
R Core Team, 2020. R: A Language and Environment for Statistical Computing. R Foundation for Statistical Computing, Vienna, Austria.
Reagan-Shaw, S., Nihal, M., Ahmad, N., 2008. Dose translation from animal to human studies revisited. Faseb. J. 22 (3), 659–661.
Rehman, A.A., Ahsan, H., Khan, F.H., 2013. alpha-2-Macroglobulin: a physiological guardian. J. Cell. Physiol. 228 (8), 1665–1675.
Rooney, K.L., Domar, A.D., 2018. The relationship between stress and infertility. Dialogues Clin. Neurosci. 20 (1), 41–47.
Roth, Z., 2018. Symposium review: reduction in oocyte developmental competence by stress is associated with alterations in mitochondrial function. J. Dairy Sci. 101 (4), 3642–3654.
Rueden, C.T., Schindelin, J., Hiner, M.C., DeZonia, B.E., Walter, A.E., Arena, E.T., Eliceiri, K.W., 2017. ImageJ2: ImageJ for the next generation of scientific image data. BMC Bioinf. 18 (1), 529–554.
Russell, M.A., Leete, P., 2019. Glucocorticoids: novel agents to stimulate beta-cell neogenesis? Ann. Transl. Med. 7 (8), 166–170.
Salehi, A., Rabiei, Z., Setorki, M., 2018. Effect of gallic acid on chronic restraint stress-induced anxiety and memory loss in male BALB/c mice. Iran J Basic Med Sci 21 (12), 1232–1237.
Samad, N., Jabeen, S., Imran, I., Zulfiqar, I., Bilal, K., 2019. Protective effect of gallic acid against arsenic-induced anxiety-/depression- like behaviors and memory impairment in male rats. Metab. Brain Dis. 34 (4), 1091–1102.
Sander, M., Sussel, L., Conners, J., Scheel, D., Kalamaras, J., Dela Cruz, F., Schwitzgebel, V., Hayes-Jordan, A., German, M., 2000. Homeobox gene Nkx6.1 lies downstream of Nkx2.2 in the major pathway of beta-cell formation in the pancreas. Development 127 (24), 5533–5540.
Sasaki, H., Hamatani, T., Kamijo, S., Iwai, M., Kobanawa, M., Ogawa, S., Miyado, K., Tanaka, M., 2019. Impact of oxidative stress on age-associated decline in oocyte developmental competence. Front. Endocrinol. 10, 811–817.
Sayegh, R.A., Tao, X.J., Leykin, L., Isaacson, K.B., 1997. Endometrial alpha-2 macroglobulin; localization by in situ hybridization and effect on mouse embryo development in vitro. J. Clin. Endocrinol. Metab. 82 (12), 4189–4195.
Schaffer, A.E., Taylor, B.L., Benthuysen, J.R., Liu, J., Thorel, F., Yuan, W., Jiao, Y., Kaestner, K.H., Herrera, P.L., Magnuson, M.A., May, C.L., Sander, M., 2013. Nkx6.1 controls a gene regulatory network required for establishing and maintaining pancreatic Beta cell identity. PLoS Genet. 9 (1) e1003274-1003288.
Schelp, F.P., Kraiklang, R., Muktabhant, B., Chupanit, P., Sanchaisuriya, P., 2019. Public health research needs for molecular epidemiology and to emphasize homeostasis - could the omnipotent endopeptidase inhibitor alpha-2-macroglobulin be a meaningful biomarker? F1000Res 8, 1025–1034.
Shannon, P., Markiel, A., Ozier, O., Baliga, N.S., Wang, J.T., Ramage, D., Amin, N., Schwikowski, B., Ideker, T., 2003. Cytoscape: a software environment for integrated models of biomolecular interaction networks. Genome Res. 13 (11), 2498–2504.
Sharma, R.K., Azeem, A., Agarwal, A., 2013. Spindle and chromosomal alterations in metaphase II oocytes. Reprod. Sci. 20 (11), 1293–1301.
Shkolnik, K., Tadmor, A., Ben-Dor, S., Nevo, N., Galiani, D., Dekel, N., 2011. Reactive oxygen species are indispensable in ovulation. Proc. Natl. Acad. Sci. U. S. A. 108 (4), 1462–1467.
Slozina, N.M., Neronova, E.G., 1990. Chromosomal disorders in the oocytes of rats after stress exposure in the preovulatory period. Tsitol. Genet. 24 (3), 37–40.
Suarez-Pozos, E., Thomason, E.J., Fuss, B., 2020. Glutamate transporters: expression and function in oligodendrocytes. Neurochem. Res. 45 (3), 551–560.
Sun, Q.Y., Schatten, H., 2006. Regulation of dynamic events by microfilaments during oocyte maturation and fertilization. Reproduction 131 (2), 193–205.
Szklarczyk, D., Gable, A.L., Lyon, D., Junge, A., Wyder, S., Huerta-Cepas, J., Simonovic, M., Doncheva, N.T., Morris, J.H., Bork, P., Jensen, L.J., Mering, C.V., 2019. STRING v11: protein-protein association networks with increased coverage, supporting functional discovery in genome-wide experimental datasets. Nucleic Acids Res. 47 (D1), D607–D613.
Tang, Y., 2006. Kai Yu Zhong Yu decoction in treating 67 cases of infertility. Yunan Journal of Traditional Chinese Medicine and Materia Medica 66–67, 06.
Tao, W., Wang, H., Su, Q., Chen, Y., Xue, W., Xia, B., Duan, J., Chen, G., 2016. Paeonol attenuates lipopolysaccharide-induced depressive-like behavior in mice. Psychiatr. Res. 238, 116–121.
The gene Ontology Consortium, 2019. The gene ontology resource: 20 years and still GOing strong. Nucleic Acids Res. 47 (D1), D330–d338.
Toufexis, D., Rivarola, M.A., Lara, H., Viau, V., 2014. Stress and the reproductive axis. J. Neuroendocrinol. 26 (9), 573–586.
Valsamakis, G., Chrousos, G., Mastorakos, G., 2019. Stress, female reproduction and pregnancy. Psychoneuroendocrinology 100, 48–57.
Victoria, M., Labrosse, J., Krief, F., Cedrin-Durnerin, I., Comtet, M., Grynberg, M., 2019. Anti Mullerian Hormone: more than a biomarker of female reproductive function. J Gynecol Obstet Hum Reprod 48 (1), 19–24.
Vogtle, F.N., Brandl, B., Larson, A., Pendziwiat, M., Friederich, M.W., White, S.M., Basinger, A., Kucukkose, C., Muhle, H., Jahn, J.A., Keminer, O., Helbig, K.L., Delto, C.F., Myketin, L., Mossmann, D., Burger, N., Miyake, N., Burnett, A., van Baalen, A., Lovell, M.A., Matsumoto, N., Walsh, M., Yu, H.C., Shinde, D.N., Stephani, U., Van Hove, J.L.K., Muller, F.J., Helbig, I., 2018. Mutations in PMPCB encoding the catalytic subunit of the mitochondrial presequence protease cause neurodegeneration in early childhood. Am. J. Hum. Genet. 102 (4), 557–573.
von Mengden, L., Klamt, F., Smitz, J., 2020. Redox biology of human cumulus cells: basic concepts, impact on oocyte quality, and potential clinical use. Antioxidants Redox Signal. 32 (8), 522–535.
Wang, C., 2003. Kai Yu Zhong Yu decoction for the treatment of female infertility experience. Shandong J. Tradit. Chin. Med. 283, 05.
Wang, X., Fang, H., Huang, Z., Shang, W., Hou, T., Cheng, A., Cheng, H., 2013. Imaging ROS signaling in cells and animals. J. Mol. Med. (Berl.) 91 (8), 917–927.
Wen, Z., Hou, W., Wu, W., Zhao, Y., Dong, X., Bai, X., Peng, L., Song, L., 2018. 6'-O-Galloylpaeoniflorin attenuates cerebral ischemia reperfusion-induced neuroinflammation and oxidative stress via PI3K/Akt/Nrf2 activation. Oxid Med Cell Longev, 2018, 8678267-8678280.
Willner, P., 2017. The chronic mild stress (CMS) model of depression: history, evaluation and usage. Neurobiol Stress 6, 78–93.
Willner, P., Towell, A., Sampson, D., Sophokleous, S., Muscat, R., 1987. Reduction of sucrose preference by chronic unpredictable mild stress, and its restoration by a tricyclic antidepressant. Psychopharmacology (Berlin) 93 (3), 358–364.
Xu, H.X., Lin, S.X., Gong, Y., Huo, Z.X., Zhao, C.Y., Zhu, H.M., Xi, S.Y., 2020. Chaiyu-dixian formula exerts protective effects on ovarian follicular abnormal development in chronic unpredictable mild stress (CUMS) rat model. Front. Pharmacol. 11, 245–262.
Yohn, C.N., Gergues, M.M., Samuels, B.A., 2017. The role of 5-HT receptors in depression. Mol. Brain 10 (1), 28–39.
Zhang, Z., 1983. Kai Yu Zhong Yu decoction in treating 30 cases of infertility of liver qi stagnation type. Shandong Med. J. 35, 03.
Zhang, M.H., Feng, L., Zhu, M.M., Gu, J.F., Wu, C., Jia, X.B., 2013. Antioxidative and anti-inflammatory activities of paeoniflorin and oxypaeoniflora on AGEs-induced mesangial cell damage. Planta Med. 79 (14), 1319–1323.
Zhang, Z., Deng, T., Wu, M., Zhu, A., Zhu, G., 2019. Botanicals as modulators of depression and mechanisms involved. Chin. Med. 14, 24–33.
Zhang, H., Zhang, S., Hu, M., Chen, Y., Wang, W., Zhang, K., Kuang, H., Wang, Q., 2020. An integrative metabolomics and network pharmacology method for exploring the effect and mechanism of Radix Bupleuri and Radix Paeoniae Alba on anti-depression. J. Pharmaceut. Biomed. Anal. 189, 113435.
Zhou, P., Lian, H.Y., Cui, W., Wei, D.L., Li, Q., Liu, Y.X., Liu, X.Y., Tan, J.H., 2012. Maternal-restraint stress increases oocyte aneuploidy by impairing metaphase I spindle assembly and reducing spindle assembly checkpoint proteins in mice. Biol. Reprod. 86 (3), 81 article 83.
Zhou, W., Ma, D., Tan, E.K., 2020. Mitochondrial CHCHD2 and CHCHD10: roles in neurological diseases and therapeutic implications. Neuroscientist 26 (2), 170–184.